

Stern and R. A. Ferrel, *ibid.* 120, 130 (1960); W. H. Weber and M. B. Webb, *ibid.* 177, 1103 (1969).

<sup>14</sup>E. G. Wilson and S. A. Rice, *Phys. Rev.* 145, 55 (1966).

<sup>15</sup>G. Holzwarth and H. J. Meister, *Tables of Asymmetry, Cross Section, and Related Functions for Mott Scattering of Electrons by Screened Gold and Mercury Nuclei* (München, 1964).

<sup>16</sup>The liquid and gas data used in these fits were taken at incident electron energies which may have been different by as much as 2% owing to voltmeter calibration. Interpolation of the gas data showed that, for such energy shifts, the changes in the gas data were smaller than the uncertainties in the gas data. To determine the importance of an inner potential correc-

tion, the liquid data were interpolated to an energy 11.6 eV below the gas data and refraction was included in the model calculation. The fits were essentially unchanged.

<sup>17</sup>J. J. Lander, *Progr. Solid State Chem.* 2, 26 (1965).

<sup>18</sup>H. Raether (private communication).

<sup>19</sup>J. J. Lander and J. Morrison, *J. Appl. Phys.* 34, 3517 (1963).

<sup>20</sup>G. Gafner, in *The Structure and Chemistry of Solid Surfaces*, edited by G. A. Somorjai (Wiley, New York, 1969).

<sup>21</sup>H. E. Farnsworth, *Phys. Rev.* 49, 605 (1936); P. W. Palmberg and T. N. Rhodin, *J. Appl. Phys.* 39, 2425 (1968); W. H. Weber and M. B. Webb, *Phys. Rev.* 177, 1103 (1969).

## Photoemission and Optical Studies of Cu-Ni Alloys. I. Cu-Rich Alloys\*

D. H. Seib<sup>†</sup> and W. E. Spicer

*Stanford University, Stanford, California 94305*

(Received 24 October 1969; revised manuscript received 23 April 1970)

Photoemission and optical reflectivity measurements of Cu-rich Cu-Ni alloys are reported. The results for alloys of composition 87% Cu-13% Ni and 77% Cu-23% Ni give conclusive evidence that a virtual bound state rather than a rigid-band model is appropriate for describing the Ni *d* states in Cu-Ni alloys. In these alloys, the Cu *d* states are found to be little changed in energy position from the *d* states in pure Cu. From the photoemission data, the Ni virtual bound state is found to be centered 0.95 eV below the Fermi energy, and the half-width at half-maximum of the state, due to *s-d* interactions alone, is found to be  $0.42 \pm 0.05$  eV. For the alloy compositions studied, it is also found that interactions among Ni states on different atoms give a significant contribution to the total width of the state. The behavior of alloy reflectivity data and optical parameters, which are deduced by a Kramers-Krönig analysis, is consistent with the alloy electronic structure obtained from the photoemission measurements.

### I. INTRODUCTION

The electronic structure and related properties of the alloys of copper with nickel have long been the subject of much theoretical and experimental interest. Cu-Ni alloys have often been taken to be the prototype of the many noble-metal-transition-metal systems, which involve the interaction of metals whose properties (at least near the Fermi surface) are determined by *s-p* derived electron states and *d*-derived electron states, respectively. In addition, Cu-Ni alloys are ferromagnetic over more than one-half of the composition range and are (ideally) substitutional solid solutions over the entire composition range. These properties, and the fact that pure Cu and pure Ni are among the best understood of the noble and transition metals, have stimulated a great amount of work on the Cu-Ni alloy system.

Early magnetic moment<sup>1</sup> and optical data<sup>2</sup> for Cu-Ni alloys led Mott<sup>3</sup> to propose in 1935 the rigid-

or common-band model of alloying behavior. The rigid-band model assumes that there is one electronic density-of-states function which is the same for Ni, Cu, and Cu-Ni alloys, with this density of states filled to an energy level determined by the electron-to-atom ratio. This model appears to still enjoy fairly wide acceptance.<sup>4</sup> However, many subsequent measurements have questioned the applicability of the rigid-band model to Cu-Ni alloys<sup>5-14</sup> and alternative models have been suggested.<sup>15,16</sup> In particular, it has been suggested<sup>10-14</sup> that a virtual-bound-state type of model, as developed by Friedel<sup>17</sup> and Anderson,<sup>18</sup> is appropriate for describing the electronic structure of Cu-rich Cu-Ni alloys.

These two different models - the rigid-band and the virtual-bound-state (VBS) models - predict quite different behavior for the density of states in Cu-Ni alloys. This is illustrated in Fig. 1. The drawing on the left-hand side of Fig. 1 illustrates schematically the optical density of states of pure

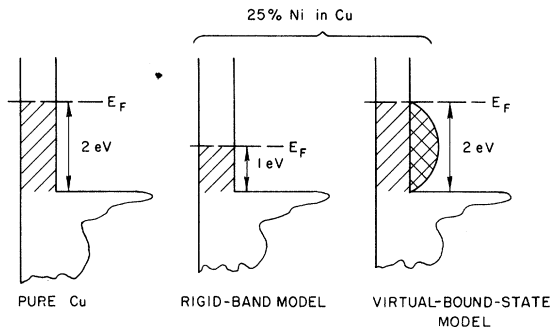


FIG. 1. Illustration of the filled density of states in Cu and Cu-Ni alloys, showing behavior expected from rigid-band and VBS models at 25% Ni in Cu.

Cu as obtained from photoemission measurements.<sup>19, 20</sup> The Cu density of states is characterized by a high density of  $d$ -derived states, for energies greater than 2 eV below the Fermi level ( $E_F$ ), and a relatively lower density of  $s$ - and  $p$ -derived states between the  $d$  states and  $E_F$ . The rigid-band model for Cu-Ni alloys assumes that when Ni is added to Cu, electrons from the  $s$ - and  $p$ -derived states fill the Ni  $d$  shell, thereby decreasing the  $E_F$  to  $d$ -state energy separation. For 25% Ni in Cu, the alloy density of states would be as shown schematically in the central drawing of Fig. 1 – the  $d$ -state to  $E_F$  separation would be decreased to about 1 eV but the total density of states would not be changed in shape.

The VBS model<sup>17, 18</sup> is appropriate for describing the states of a  $3d$  transition-metal impurity atom in a host metal with a nearly free-electron-like band. The essence of this model is that the impurity  $3d$  orbitals form levels, highly localized around the impurity atom, that are broadened in energy around  $E_d$ , the center of the state, through a resonant scattering interaction with the nearly free-electron-like band of the host metal. In a noble-metal host (which contains both  $s$ -,  $p$ -, and  $d$ -derived states) if the  $d$ -state scattering resonances of the host and impurity metals are well separated in energy, as might be expected for Ni in Cu, then the situation shown schematically in the right-hand portion of Fig. 1 would result. Cu and Ni  $d$  electrons would form essentially independent levels, the copper  $d$ -state to  $E_F$  energy separation would be essentially unchanged, and the Ni  $d$  electrons would cause an increase in the alloy density of states between the Cu  $d$  states and  $E_F$ .

We report and discuss here photoemission and optical measurements of Cu-Ni alloys which show conclusively that a VBS type of model is appropriate for describing these alloys. Photoemission

measurements, by giving information concerning transition probabilities from states at a given initial energy, can give a direct measure of the density of states at energies well separated from the Fermi energy. Hence, such measurements can easily distinguish between the behavior predicted by the rigid-band and VBS models (Fig. 1). The relatively good energy resolution of photoemission experiments (the effective broadening function has a half-width of 0.2 to 0.3 eV) enables the changes in density-of-states structure occurring upon alloying to be readily observed. The photoemission measurements described here not only indicate the correctness of the VBS model for Cu-Ni alloys but allow an estimate of the position and width of the VBS and the variation of these quantities with increasing Ni concentration to be made. Optical measurements (the measurement of the total optical absorption as a function of energy), such as have been made previously for Cu-Ni alloys,<sup>11, 14</sup> also probe states well removed from  $E_F$ , but the difficulty of separating out the many different contributions to the total absorption greatly complicates obtaining accurate quantitative information about the changes in density-of-states structure which occur upon alloying.

Preliminary accounts of some of this work have been given previously.<sup>21</sup> In addition to a presentation of new and improved data, a more complete analysis and discussion is now given. In the following paper,<sup>22</sup> data for Ni-rich Cu-Ni alloys and alloys of intermediate composition are presented and discussed.

## II. CLUSTERING IN Cu-Ni ALLOYS

Before embarking upon a presentation and discussion of the photoemission data for Cu-Ni alloys, deviations from ideal solid solution behavior in this alloy system and the implications these deviations might have on the interpretation of optical and photoemission data must be examined.

Recently, considerable attention has been focused upon the nature and extent of short-range ordering and clustering in Cu-Ni alloys. One of the most quantitative characterizations of the clustering has been given by Mozer, Keating, and Moss,<sup>23</sup> who measured the cluster diffuse neutron scattering from a specially prepared sample of composition 52.5% Cu-47.5% Ni and deduced the short-range order parameters  $\alpha_i$ . The measurements indicated that there is a fairly small tendency for Cu and Ni atoms in a Cu-Ni alloy to prefer nearest neighbors of the same atomic species, but beyond the nearest-neighbor shell the atomic arrangement is essentially random. Specifically, for the alloy containing 47.5% Ni,  $\alpha_1$  was found to be 0.121,

implying that the probability for finding a Ni atom in the first-neighbor shell around a Ni atom is 0.539 instead of 0.475. The deduced short-range-order parameters are characteristic of the alloy at  $\sim 550^\circ\text{C}$ , since any reasonable quenching of an alloy specimen from high temperatures freezes in the atomic arrangements at this temperature.<sup>23</sup> In another measurement of short-range-order parameters, Cable, Wollan, and Child<sup>24</sup> found that  $\alpha_1 \cong 0.05$  for an 80% Ni-20% Cu alloy. These authors also show that  $\alpha_1$  should vary as  $c(1-c)$ , where  $c$  is equal to concentration of one atomic species, indicating less tendency toward clustering for alloys with compositions near pure Cu or pure Ni.

Measurements of the magnetic susceptibilities of Cu-rich Cu-Ni alloys also give information concerning cluster effects. From such measurements it is apparent, first of all, that clustering is greatly reduced in samples which have been properly homogenized and quenched. Second, in properly prepared Cu-Ni samples, atomic clustering decreases as the Ni content decreases. Van Elst, Lubach, and Van Den Berg<sup>25</sup> reported spontaneous magnetic moments for alloys containing 40 and 30% Ni, indicating very pronounced clustering. However, the samples used by Van Elst *et al.* were annealed for only 3 h at  $900^\circ\text{C}$ , which appears to be insufficient heat treatment. Using samples given a more careful annealing treatment, Ryan, Pugh, and Smoluchowski<sup>26</sup> observed superparamagnetic behavior in the susceptibilities of alloys with composition near 40% Ni. That is, the susceptibilities behaved as if there were (within the homogeneous, unclustered material) small clusters of material sufficiently rich in Ni to be ferromagnetic. Roy and Subrahmanyam<sup>27</sup> did not find, in alloys containing 42 and 52% Ni, the strong superparamagnetism reported by Ryan *et al.* for alloys of similar composition.

For alloys with Ni concentrations less than about 30%, Ryan *et al.*<sup>26</sup> found that the magnetic susceptibilities were temperature independent, implying that regions sufficiently rich in Ni to have spontaneous magnetic moments do not exist in these compositions in properly homogenized samples. Robbins, Claus, and Beck<sup>16</sup> have suggested that a Ni atom surrounded by more than seven nearest-neighbor Ni atoms will have a magnetic moment. This is about twice the number of Ni nearest neighbors that would be expected on an average basis for Ni concentrations less than 30%. Therefore, the absence of paramagnetism in alloys containing less than 30% Ni suggests that the clustering and short-range-order effects which might be present do not lead to appreciable numbers of Ni atoms with this number of Ni nearest neighbors. Certainly the magnetic data exclude the possibility that large

clusters of almost pure Ni could exist in alloys containing up to 30% Ni.

Neutron-diffraction measurements, made by Hicks, Rainford, Kouvel, Low, and Comly,<sup>28</sup> have indicated that in Cu-Ni alloys with composition near the critical composition for ferromagnetism, the sample magnetization is distributed in giant magnetic polarization clouds of about  $8-\mu_B$  total moment. These polarization clouds, which arise on a statistical basis or due to short-range-order effects, may explain the apparent atomic clustering found in the magnetic-susceptibility measurements<sup>26</sup> and in alloy specific-heat measurements.<sup>7,9,16</sup> In Mössbauer studies of the magnetic polarization cloud formed around isolated Fe atoms in Cu-Ni alloys, Bennett, Swartzendruber, and Watson<sup>29</sup> have found that there is very little or no deviation from randomness in homogenized and rapidly quenched Cu-Ni alloy specimens.

Kidron<sup>4</sup> has concluded from the magnetic-susceptibility data of Ryan *et al.*<sup>26</sup> and his own small-angle x-ray diffraction data that clusters containing 70% Ni atoms exist in a 50% Cu-50% Ni alloy and constitute 18 to 55% of the volume of the alloy specimen. The Cu-Ni sample used in Kidron's measurements was annealed at  $300^\circ\text{C}$  for 50 h. Because of this annealing treatment, which was for a temperature in the vicinity of the critical temperature for phase separation,<sup>23</sup> Moss<sup>30</sup> has concluded that Kidron's x-ray diffraction data are most likely explained by the fact that spinodal decomposition had begun. If this is true the clustering effects should not be as pronounced as Kidron has suggested in samples quenched from high temperatures and not subjected to long low-temperature annealing.

On the basis of the above discussion, we believe that clustering effects will not adversely affect photoemission data for Cu-Ni alloys containing up to 25% Ni, which are of interest here. Present evidence indicates that there can be some deviation from ideality in nearly equiatomic alloys, but such deviations are small in properly homogenized specimens and become less important for compositions near pure Ni or pure Cu. The alloy specimens used in the present photoemission and optical measurements have been homogenized and quenched, as detailed in Sec. III, in order to reduce deviations from ideality to a minimum. Heat treatments used to clean the sample surfaces prior to photoemission measurements (Sec. III) have been done for relatively short times and at temperatures well above the critical temperature for phase separation. Even if some small amount of clustering should remain in our samples the photoemission and optical results should be relatively unaffected. Regions of different composition will contribute to

photoemission and optical measurements in proportion to the relative amount of sample volume occupied. Since any remaining clusters would occupy only a very small fraction of the volume, these measurements will be dominated by the homogeneous volume. Therefore, the conclusions reached from the results below should apply to ideal unclustered Cu-Ni specimens.

### III. EXPERIMENTAL TECHNIQUES

#### A. Initial Sample Preparation

Photoemission and optical data will be reported for single-crystal alloy samples of composition 87% Cu-13% Ni and 77% Cu-23% Ni. A single-crystal copper sample was also studied to check the sample-preparation techniques used for the alloy specimens. Cu and 77% Cu crystals were obtained from Research Crystals, Inc., Richmond, Va. and the 87% Cu crystal was obtained from Aremco, Inc., Briarcliff Manor, N. Y. After receipt, the alloy crystals were subjected to a long high-temperature anneal: The 87% Cu crystal was annealed 14 days at 1000 °C in an evacuated quartz ampoule and the 77% Cu crystal was annealed 13 days at 960 °C in a continually pumped vacuum furnace. After annealing, the rods were quenched in air. Following the homogenization treatment, specimens suitable for measurement were cut from the crystal rods and smoothed using a spark-machining device. After spark machining, the samples were further smoothed by mechanical polishing. These same procedures, excepting the high-temperature anneal, were also used for the initial preparation of the pure Cu sample. The true average composition of the alloy samples was determined by quantitative chemical analysis performed by Metallurgical Laboratories, Inc., San Francisco, Calif.

In order to remove damaged surface layers resulting from the mechanical polishing step, pure Cu and 87% Cu samples were electrochemically polished in a solution of 33% nitric acid and 67% methyl alcohol.<sup>31</sup> The 77% Cu samples were chemically polished using a potassium dichromate solution<sup>32</sup>: In this case, polishing was accomplished by saturating a cotton ball with solution and swabbing over the sample. The specimen was frequently washed in running distilled water. These procedures resulted in scratch-free surfaces, although some minor pitting resulted from the electrochemical polishing procedure. Immediately after the final polishing step, the samples were mounted in the ultrahigh-vacuum measurement chamber and pumping was initiated as rapidly as possible.

Visual inspection of 77% Cu specimens after chemical polishing revealed a regular checkered pattern on the surfaces. This was a result of com-

positional inhomogeneity within the sample due to the dendritic growth process<sup>32</sup> of the crystal and the fact that the rate of attack of the polishing solution used varied slightly with alloy composition. The spacing between dendrites was approximately 1 mm. In order to obtain a quantitative measure of the magnitude of the compositional variation, a microprobe analysis was made on one 77% Cu sample. This analysis was generously performed by Dils, using the facilities of Pratt and Whitney Aircraft Co., Middletown, Conn. The microprobe analysis (which has spatial resolution of about 3  $\mu$ ) showed that there was indeed a measurable composition difference across the surface of the sample which coincided with the visible dendritic pattern. The distribution of Ni concentrations within the sample was very nearly symmetrical about the average Ni content. The actual Ni content in the sample ranged from 17 to 30%, although about 90% of the sample had Ni concentrations between 19 and 28% and about 70% of the sample corresponded to Ni concentrations between 21 and 25.7%.

#### B. Heat Cleaning of Samples

Since the Cu and alloy sample surfaces were subject to atmospheric contamination before mounting in the high-vacuum photoemission measurement chamber, a means of cleaning the surfaces in vacuum was required. This cleaning was accomplished by heating the samples in vacuum. Heat treatment at 500-600 °C for a total of about 10 h was found to give clean surfaces, as judged by the quality of the photoemission results themselves.

The major contaminants on the Cu and Cu-Ni alloy surfaces are probably oxides. While it has been suggested that heating will remove oxides from Cu surfaces,<sup>33,34</sup> it is questionable whether the last one or two monolayers can be removed in this manner.<sup>35</sup> However, we have found that by heating Cu samples photoemission results can be obtained which closely resemble results obtained using Cu films evaporated in ultrahigh vacuum (Sec. IV). Such evaporated films are thought to be atomically clean.<sup>20</sup> Before heat-cleaning treatments, the measured photoelectron kinetic-energy distribution curves (EDCs) for bulk samples were usually characterized by a lack of structure and by a large number of electrons with very low kinetic energies, due apparently to scattering of electrons by the surface contamination. Upon heating, the relative number of electrons with low kinetic energy diminished and structure characteristic of the density of states of the material under study appeared at higher kinetic energies. Cleaning-heat treatments were continued until the number of low-energy electrons was reduced as far as possible and until further heating resulted

in no changes in the measured EDCs. In contrast to the success of heat cleaning for pure Cu and Cu-rich Cu-Ni alloys, heat cleaning did not lead to correct photoemission results for Ni and Ni-rich Cu-Ni alloys.<sup>22</sup>

### C. Measurement Equipment and Techniques

For photoemission measurements, the samples studied and the electron energy-analyzer system were housed in stainless-steel ultrahigh-vacuum chambers. The experimental apparatus also incorporated a resistance heater for accomplishing sample surface cleaning as described above. Pressure during measurement was  $\leq 10^{-9}$  Torr, but was higher ( $\sim 10^{-8}$  Torr) during heat cleaning of the samples.

Techniques for obtaining photoemission data (energy distribution of photoemitted electrons and quantum yield) have been described previously.<sup>36,37</sup> A  $\text{Cs}_3\text{Sb}$  photodiode calibrated in this laboratory by Koyama<sup>38</sup> was used as an absolute intensity standard in order to obtain the absolute quantum yield. Photoemission measurements on clean samples have been made for photon energies from about 5 eV to the LiF cutoff at about 11.8 eV.

The near-normal-incidence reflectivities of the alloy samples (the same samples used in photoemission experiments) were obtained using the reflectivity apparatus described by Yu, Donovan, and Spicer.<sup>39</sup> The reflectivity apparatus was modified so that samples could be cleaned by heating; changes in the magnitude of the reflectivity, particularly at high energies, did occur after heating, but these changes were not as pronounced as those observed in photoemission measurements after heat cleaning. Reflectivity measurements could be made for photon energies between 1.2 and 11.8 eV in high vacuum. To extend the measurements to lower energies, the reflectivity of the samples was obtained between 0.5 and 2.0 eV using a Cary 14 spectrophotometer with specular reflectivity attachment. These measurements were made in air, immediately after the sample was removed from the high-vacuum chamber. The over-all accuracy in the reflectivity spectra, due to uncertainties in optical alignment and surface preparation, is estimated to be  $\pm 5\%$ .

## IV. ANALYSIS PROCEDURES

### A. Nondirect Model of Optical and Photoemission Processes

The alloy photoemission data to be presented below will be discussed in terms of the nondirect-transition model formulated by Spicer and co-workers.<sup>19,20,40</sup> The central assumption of this model is that optical transition probabilities are determined by a product of initial and final den-

sities of states and do not depend strongly upon the wave vector  $\vec{k}$ . The nondirect-transition model predicts that structure in EDCs due to structure in the filled density of states of a material obeys the relation  $\Delta E_s = \Delta h\nu$ , where  $\Delta E_s$  is the change in energy position of EDC structure and  $\Delta h\nu$  is the change in photon energy. Structure is also expected to vary smoothly with changing  $h\nu$ . A large amount of experimental photoemission data for metals (and other classes of solids as well) has been found to behave in this manner. In particular, photoemission data for pure Cu<sup>19,20</sup> and pure Ni<sup>41</sup> have been found to agree well with the predictions of the nondirect-transition model.

The question of whether transitions from the  $d$ -derived states of Cu do or do not conserve one-electron wave vectors  $\vec{k}$  is still somewhat controversial, particularly since recent calculations of EDCs for pure Cu by Smith and Spicer<sup>42</sup> using a direct-transition assumption have shown that the predictions of both the direct and nondirect models have certain features in common. In photoemission studies of cesiated Cu films, Smith and Spicer<sup>42</sup> have found evidence for some direct transitions from the  $d$ -derived states of Cu. Spicer<sup>43</sup> has recently attempted to put these results in perspective.

The nondirect model is preferred for the analysis of our alloy photoemission data for several reasons. Structure observed in the alloy data exhibits the behavior predicted by the nondirect model; structure obeys the relation  $\Delta E_s = \Delta h\nu$  and varies smoothly in magnitude with different  $h\nu$ . In an alloy system, the lack of potential periodicity implies that the energy eigenstates cannot be associated with a single  $k$  value. Particularly in a strong scattering situation, or a situation in which certain states are predominately confined to one of the constituent species and excluded from the other, which will be found to be the case for the Ni and Cu  $d$  states in the Cu-Ni system, the resultant, necessary distortion of the wave functions describing these states implies that  $\vec{k}$  will not be a meaningful quantum number. Hence conservation of one-electron  $\vec{k}$  and direct transitions will tend to lose their meaning in such a system. Certainly  $\vec{k}$  conservation will not be meaningful for transitions involving the states of dilute solute atoms, such as the  $d$  states of Ni in Cu discussed below. In Cu-rich Cu-Ni alloys, we have found<sup>21</sup> no evidence for the direct  $L'_2 \rightarrow L_1$  transition, which is observed in pure Cu.<sup>19</sup> Finally, Doniach<sup>44</sup> has examined the effects of many-body screening of the valence hole in the uv optical excitation process. Preliminary results suggest that such effects can produce a spread in the possible  $\vec{k}$  values of an optical excitation event. The spread in  $k$  increases as the effective mass of the hole increases. Such effects appear to be im-

portant in the relatively flat  $d$ -derived bands of Cu, and the spread in  $\vec{k}$  would be expected to increase with any tendency of the Cu  $d$  bands to narrow as Cu is alloyed with Ni. These considerations indicate that the nondirect-transition model is the logical starting point for analysis of our alloy data.

By using the nondirect-transition model and certain other simplifying assumptions, Berglund and Spicer<sup>19</sup> and Krolikowski and Spicer<sup>20</sup> have given expressions for the photoelectron EDCs in terms of the density of states of a material. The contributions of various scattering mechanisms to the EDCs have been given by Berglund and Spicer.<sup>19</sup> The expression for  $N(E, h\nu)$ , the number of electrons photoemitted at energy  $E$  (above the Fermi energy) for a photon energy  $h\nu$ , including the contribution of once inelastically (electron-electron) scattered electrons is

$$N(E, h\nu) = \frac{T(E)\alpha l_e(E)|M|^2}{\omega\sigma(h\nu)[1+\alpha l_e(E)]} \left\{ N_i(E-h\nu)N_f(E) + \int_E^{h\nu} N_i(E'-h\nu)N_f(E') \frac{s_e(E', E)}{S_e(E')} \times \left[ \frac{\ln[1+\alpha l_e(E')]}{\alpha l_e(E')} + \frac{l_e(E)}{l_e(E')} \ln\left(1 + \frac{l_e(E')}{l_e(E)}\right) \right] dE' \right\} \quad (1)$$

In this equation the first term in curly brackets is due to primary (unscattered) electrons and the second term is the contribution of electrons scattered by electron-electron (inelastic) processes. In Eq. (1),  $N_i(E)$  is equal to the optical density of filled states,  $N_f(E)$  is equal to the optical density of empty states,  $\alpha$  is the optical absorption coefficient (a function of  $h\nu$ ), and  $T(E)$  is the energy-dependent escape function for electrons arriving at the sample surface.  $|M|^2$  is the square of the optical matrix element connecting initial and final states. It is taken to be constant with respect to final-state energy and photon energy.<sup>20,41</sup> The mean free path for electron-electron (inelastic) scattering is  $l_e(E)$  and  $s_e(E')$  and  $S_e(E')$  are electron-electron scattering probabilities.<sup>19</sup> Berglund and Spicer have given a method for calculating the electron-electron mean free path and scattering probabilities from the density of states.

The term  $\omega\sigma(h\nu)$  (the optical transition strength) in Eq. (1) is proportional to the total number of transitions taking place per unit time, therefore dividing by  $\omega\sigma(h\nu)$  normalizes the expression for  $N(E, h\nu)$  to be the number of electrons emitted at energy  $E$  per absorbed photon. In terms of the nondirect-transition model,  $\omega\sigma(h\nu)$  can be simply expressed in terms of the densities of states (see below). Therefore, Eq. (1) specifies the EDCs completely in terms of the density of states of a material, certain optical parameters, and the

assumptions of the nondirect-transition model.

Krolikowski and Spicer<sup>20</sup> have given a procedure for extracting the optical density of initial states of a metal by using experimental photoemission data, the first part of Eq. (1), and several additional assumptions. In this procedure, which was successfully applied to Cu,<sup>20</sup> the optical density of empty states and the escape probability were taken to be given by a free-electron model, and the magnitude of the electron-electron scattering mean free path was determined by fitting the experimental quantum yield. The filled optical density of states was estimated from the photoemission data, and EDCs were calculated using Eq. (1). The parameters of the model were then adjusted and fine adjustments made to the filled density of states until the best agreement of experimental and calculated EDCs was obtained. We have used the same approach here to deduce the optical densities of filled states for the Cu-Ni alloys studied. The contribution to the EDCs of once-scattered electrons due to electron-electron collision processes has also been included in the present analysis.

The derivation of Eq. (1) assumes  $l_e \ll l_p$ , where  $l_p$  is the elastic or electron-phonon scattering mean free path. This relationship is valid in pure noble or transition metals for the energies of interest but is not necessarily satisfied in an alloy because the elastic mean free path may be greatly reduced due to the disorder of the alloy system. In obtaining the density of filled states for 77% Cu, a modified form of Eq. (1), which included an escape probability function given by Duckett<sup>45</sup> that incorporates both the effects of elastic and inelastic scattering, was used. However, the differences between EDCs calculated using  $l_p = 30 \text{ \AA}$ , the elastic scattering mean free path found to be appropriate for 77% Cu and  $l_p = \infty$ , were not significant. This indicates that for the alloys studied here inelastic scattering effects remain much more important than elastic scattering processes in determining the photoemission data.

The densities of states obtained from the nondirect-transition model using the above procedures are properly referred to as "optical densities of states," and this term will be used in subsequent discussions. That is, the deduced densities of states are appropriate for understanding photoemission data and, because of the assumption of constant optical matrix elements, may differ from the true electronic densities of states. In experiments on many metals, matrix elements appear to be relatively constant with  $h\nu$  and final-state energy, but different initial states, for instance, the  $s$ - and  $p$ -derived and the  $d$ -derived states of Cu, may have different matrix elements when coupled to the same final states. Hence, the constant-matrix-

element assumption of the nondirect-transition model may not give the true relative strengths of structure in the actual electronic density of states. The reasonable agreement (particularly with regard to the energy location of peaks in the density of states) that has been found between the optical densities of states for Ni<sup>41</sup> and Cu<sup>20</sup> and the band-structure densities of states<sup>46,47</sup> suggests that the optical density of states is quite representative of the true density of states in these and similar materials.

In the nondirect constant-matrix-element model, the optical transition strength  $\omega\sigma$  (equal to  $\omega^2\epsilon_2/4\pi$  in cgs emu, with  $\epsilon_2$  the imaginary part of the complex dielectric constant) can be expressed as

$$\omega\sigma(h\nu) = |M|^2 \int_{E_F}^{E_F+h\nu} N_i(E-h\nu)N_f(E)dE \quad (2)$$

Here  $|M|^2$ ,  $N_i$ , and  $N_f$  have the same definitions as above;  $|M|^2$  is taken to be constant with respect to  $E$  and  $h\nu$ , and  $E_F$  is the Fermi energy. Use of Eq. (2) to calculate  $\omega\sigma$  from the optical density of states obtained from photoemission data for comparison to the measured  $\omega\sigma$  can serve as a check on the assumptions of the nondirect analysis, particularly the assumption of constant optical matrix elements. It will be suggested in the following paper that, while  $|M|^2$  does appear to be constant for the range of photon and final-state energies used in photoemission measurements, some variations in optical matrix elements do occur for certain transitions in Cu, Ni, and Cu-Ni alloys with lower final-state energies.

#### B. Derivation of Optical Parameters

Optical parameters for Cu-Ni alloys have been obtained from measured reflectivity spectra by using a Kramers-Krönig analysis.<sup>48</sup> At low photon energies, the reflectivity was taken to vary smoothly between 100% at  $h\nu=0$  and the last measured datum point at  $h\nu=0.5$  eV. The deduced optical parameters for  $h\nu>0.5$  eV were not affected by different, reasonable, low-energy extrapolations. For energies greater than the final measured datum point, the reflectivity was taken to vary as  $R \propto (h\nu)^{-2}$ ; a self-consistency procedure was used to determine the best value of  $p$ .<sup>49</sup> Different values of  $p$  do not affect the position and shape of structure in the deduced optical parameters but do affect the magnitude of the parameters.<sup>39</sup>

Because of errors in the original reflectivity data and uncertainties in the Kramers-Krönig analysis procedure, the over-all accuracy in magnitude of the calculated optical parameters is estimated to be about  $\pm 20\%$ . In the present work, the major interest is in the comparison of optical parameters for different alloy compositions to ascertain the changes which occur upon alloying. The same value of the parameter  $p$  was used to extrapolate the re-

flectivity data for all alloys studied, indicating that such comparisons of the calculated optical parameters can be made with confidence.

### V. EXPERIMENTAL RESULTS

#### A. Photoemission from Pure Cu

EDCs for pure Cu at an exciting photon energy of 10.2 eV are shown in Fig. 2. The solid curve shows the EDC obtained in the present work using a bulk heat-cleaned sample of Cu; the dashed curve was obtained by Krolikowski and Spicer<sup>20</sup> from an evaporated Cu film. The EDCs of Fig. 2 are plotted on the horizontal axis versus the initial-state energy,  $E_i = E - h\nu + \phi$ , where  $E$  is the kinetic energy of the photoelectrons,  $h\nu$  is the photon energy, and  $\phi$  is the sample work function. Plotting the curves in this way refers the photoemitted electrons to the energies of their initial states; this representation of the data is particularly convenient when structure in the EDCs is due to structure in the filled states and the nondirect-transition model applies, for in this case structure in EDCs for different  $h\nu$  superimposes in initial-state energy. The zero of initial-state energy corresponds to the Fermi energy (to within about 0.1 eV). The vertical scale of Fig. 2 gives the number of electrons photoemitted per absorbed photon per electron volt, that is, the curves are normalized to their respective quantum yields (the yield for the bulk Cu sample is shown in Fig. 3). Unless otherwise noted, all EDCs to be presented below will be plotted in the above manner - normalized to the quantum yield and versus

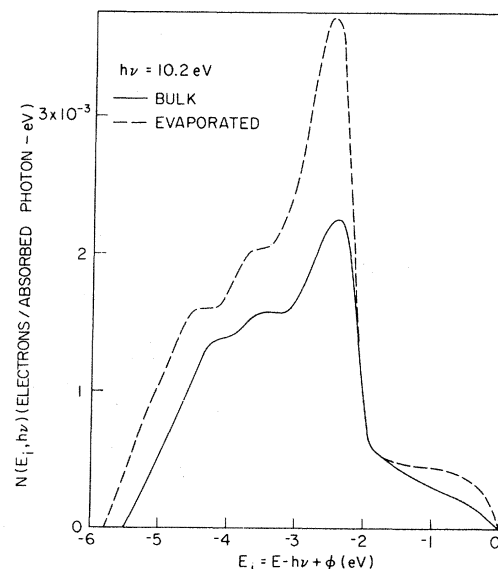


FIG. 2. Comparison of EDCs for bulk heat-cleaned Cu and for evaporated film (Ref. 20). Structure in the two EDCs is essentially identical in energy position.

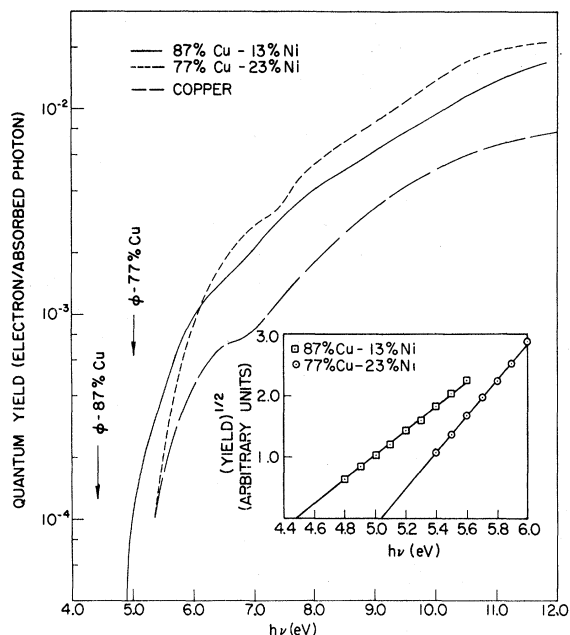


FIG. 3. Absolute quantum yields for Cu and 87% Cu and 77% Cu Cu-Ni alloys. Insert shows Fowler plots for alloy data.

the initial-state energy.

We have given a comparison of EDCs for bulk and evaporated Cu samples at only one photon energy; however, the similarities and difference between the two EDCs of Fig. 2 are typical of the similarities and differences in all other EDCs obtained for the two different Cu samples. The energy position and shape of structure in the EDCs of Fig. 2 is essentially identical. The difference in absolute magnitude of the two EDCs results because the quantum yields of the two types of Cu samples were different; the yield of the evaporated film was greater than that of the bulk sample. The basic over-all agreement of the two EDCs does suggest that adequate photoemission results can be obtained from bulk samples with surfaces prepared by heat cleaning.

Krolikowski and Spicer<sup>20</sup> have discussed in detail the structure observed in EDCs for pure Cu. It is sufficient here to note that structure in the EDCs of Fig. 2 is due to structure in the filled density of states of Cu. Between 0 and -2.0 eV electrons are excited from the nearly free-electron-like *s*- and *p*-derived states of Cu. The sharp edge at about -2.0 eV and structures at about -2.4, -3.55, and -4.3 eV are due to excitation of electrons from the *3d*-derived states of Cu.

#### B. Photoemission from Cu-Ni Samples

The photoemission data presented below for the

87% Cu-13% Ni alloy were obtained after heating the sample at 520 °C for 11 h, and the data for the 77% Cu-23% Ni alloy were obtained after heat treatments of 11 h at 410 °C and 5½ h at 475 °C. In both cases, additional heating did not cause significant changes in the EDCs obtained.

Figure 3 shows the absolute quantum yield for the 87% Cu and 77% Cu alloy samples. The quantum yield is calculated using the measured reflectivities of the samples (Sec. VD) in order to obtain the photoelectric yield per absorbed photon. Fowler<sup>50</sup> plots of the alloy-yield data near the threshold for photoemission are shown in the insert in Fig. 3. The work function of the 87% Cu alloy is found to be  $4.45 \pm 0.05$  eV. The 87% Cu sample surface was a {100} plane (determined by x-ray diffraction). For the 77% Cu alloy, which had a surface parallel to {311} planes, the work function is  $5.05 \pm 0.05$  eV. These values differ slightly from the value of 4.8 eV obtained from the pure Cu sample which had {100} surface orientation. At high photon energies the quantum yield is seen to increase with increasing Ni content.

Figures 4-6 show EDCs for 87% Cu-13% Ni for exciting photon energies between 6.4 and 11.6 eV. In these EDCs, five peaks are observed to superimpose in initial-state energy very well. One peak is seen at an initial-state energy of about -1.0 eV. The actual peak becomes less distinct as the photon energy increases due to the fact that the peak moves away from the rapidly varying portion of the escape function and electrons near the leading edge are lost to inelastic scattering processes. The relative number of electrons emitted for energies between 0 and -2.0 eV remains considerably

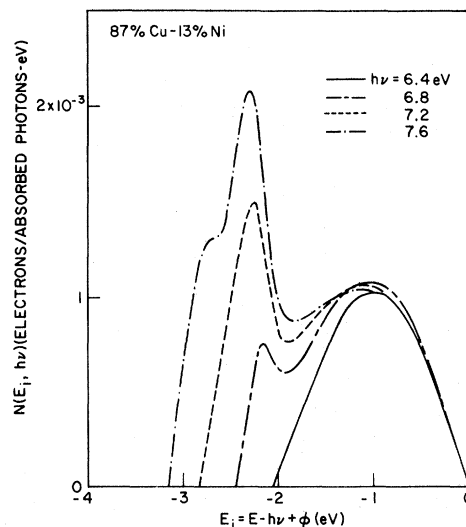


FIG. 4. EDCs for 87% Cu-13% Ni,  $6.4 \text{ eV} \leq h\nu \leq 7.6 \text{ eV}$ .



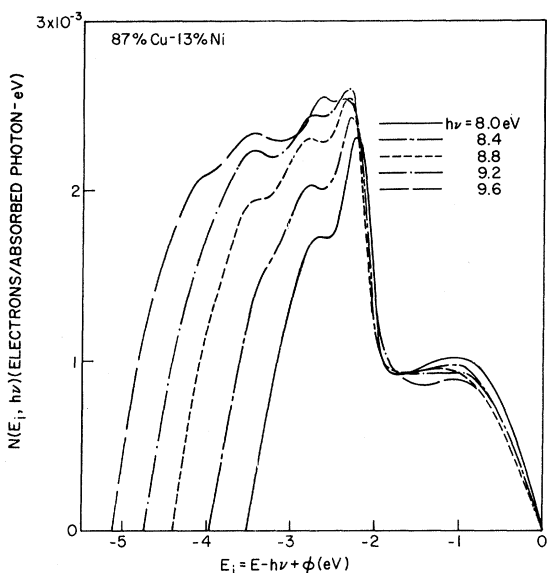


FIG. 5. EDCs for 87% Cu-13% Ni,  $8.0 \text{ eV} \leq h\nu \leq 9.6 \text{ eV}$ .

greater than in pure Cu (Fig. 2 and Ref. 20). A sharp edge occurs in the curves for initial-state energies between  $-2.0$  and  $-2.3 \text{ eV}$ . Below this edge, peaks can be distinguished at  $-2.4$ ,  $-2.7$ ,  $-3.6$ , and  $-4.4 \text{ eV}$ .

Because of the fact that structure in the EDCs of Figs. 4-6 superimposes in initial-state energy, this structure closely resembles structure in the filled density of states of 87% Cu-13% Ni. The observations of an edge near  $-2.0 \text{ eV}$ , similar to that in Cu due to the Cu  $d$  states, and the increased number of states, compared to pure Cu, between  $0$  and  $-2.0 \text{ eV}$ , are consistent with the behavior, discussed in Sec. I, expected from the VBS model,

and therefore indicate that the Ni  $d$  electrons in Cu-Ni alloys are forming virtual-bound-type states in the nearly free-electron-like states of the Cu host.

In Figs. 7-9, EDCs for the alloy of composition 77% Cu-23% Ni are shown for photon energies between  $6.0$  and  $11.6 \text{ eV}$ . Structure in the curves superimposes quite well for different  $h\nu$ . Again, a sharp distinct edge in the number of photoemitted electrons occurs at about  $-2.0 \text{ eV}$  and peaks can be identified at energies of  $-2.45$ ,  $-2.8$ ,  $-3.55$ , and  $-4.3 \text{ eV}$ . A pronounced peak is also present at  $-1.1 \text{ eV}$ , and the relative number of photoelectrons emitted for energies between  $0$  and  $-2.0 \text{ eV}$  is much greater in this alloy than in pure Cu or 87% Cu. As in the case of EDCs for 87% Cu, the curves for 77% Cu are in accord with the predictions of the VBS model rather than with the predictions of the rigid-band model.

Whereas structure between  $0$  and  $-2.0 \text{ eV}$  in the alloy EDCs is attributed to the excitation of Ni  $d$  electrons existing in virtual-bound-type levels, comparison of EDCs from 87% Cu and 77% Cu with those from pure copper indicates that structure in the alloy curves for energies less than about  $-2.0 \text{ eV}$  is due to excitation of the Cu  $d$ -derived states. This point can be established with the aid of Fig. 10, which compares EDCs for the three materials for a photon energy of  $10.2 \text{ eV}$ . The difference in absolute magnitude of the three curves results because the EDCs are normalized to their respective quantum yields, which increases with Ni content (Fig. 3). The sharp distinct rise in the number of electrons photoemitted occurs at the same energy,  $-2.0 \text{ eV}$ , in all three materials. In pure Cu, this rise is associated with the onset of transitions from the  $d$ -derived states, as discussed

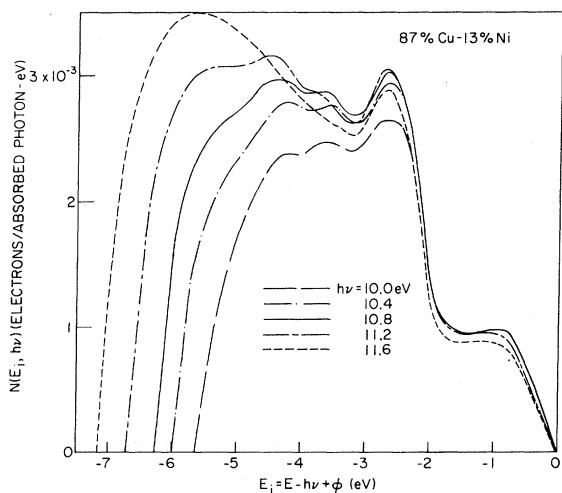


FIG. 6. EDCs for 87% Cu-13% Ni,  $10.0 \text{ eV} \leq h\nu \leq 11.6 \text{ eV}$ .

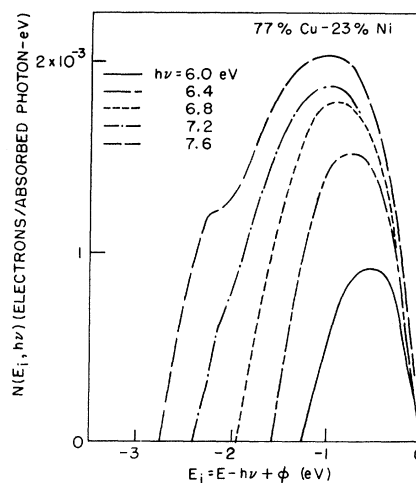


FIG. 7. EDCs for 77% Cu-23% Ni,  $6.0 \text{ eV} \leq h\nu \leq 7.6 \text{ eV}$ .

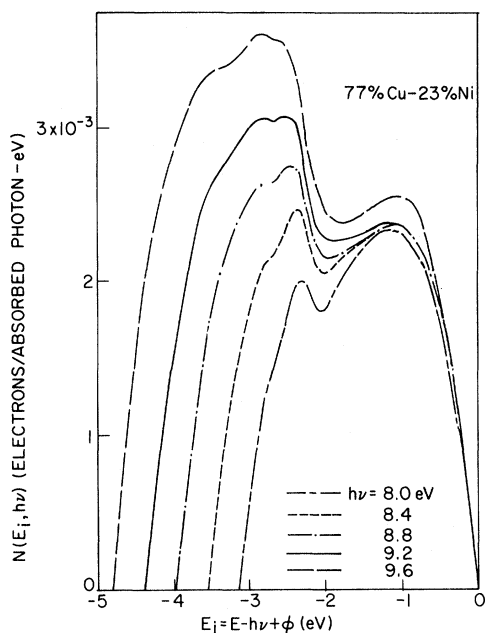


FIG. 8. EDCs for 77% Cu-23% Ni,  $8.0 \text{ eV} \leq h\nu \leq 9.6 \text{ eV}$ .

in Sec. V A. Therefore, it is natural to associate the rises in the alloy curves at the same energy with the onset of transitions from Cu  $d$ -derived states. By the same analogy, electrons emitted with energies less than  $-2.0 \text{ eV}$  are predominantly excited from the Cu  $d$ -derived states in the alloys.

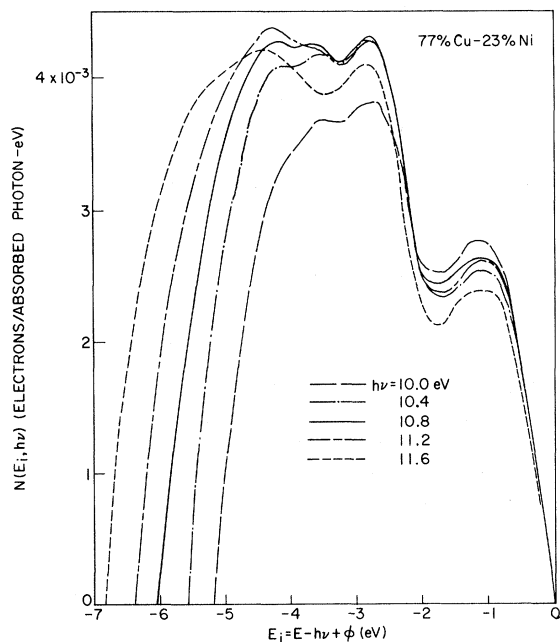


FIG. 9. EDCs for 77% Cu-23% Ni,  $10.0 \text{ eV} \leq h\nu \leq 11.6 \text{ eV}$ .

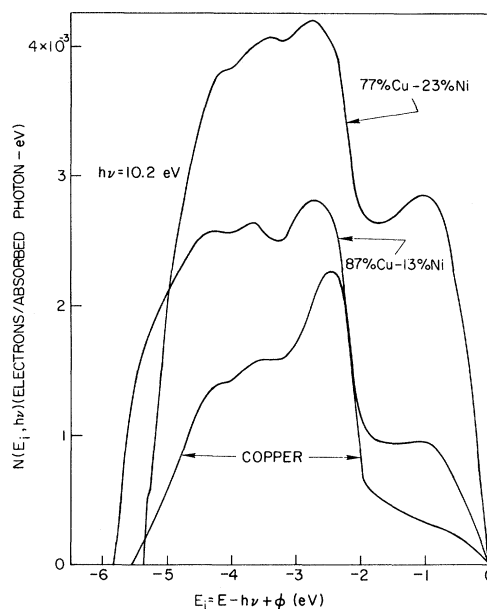


FIG. 10. Comparison of EDCs for Cu, 87% Cu, and 77% Cu. The curves are normalized to their respective yields. The energy position of structure from the Cu  $d$  states ( $E_i < -2 \text{ eV}$ ) remains constant; the buildup of structure at  $-1.0 \text{ eV}$  is due to Ni  $d$  electrons in virtual-bound-type states.

The fact that the rise occurs at the same energy in all three compositions establishes that the Cu  $d$ -state to Fermi-level energy separation is essentially unchanged upon alloying (to within the experimental resolution of about  $0.1 \text{ eV}$ ). The energy position of structure near  $-2.35$ ,  $-2.75$ ,  $-3.45$ , and  $-4.25 \text{ eV}$  also remains constant to within about  $\pm 0.1 \text{ eV}$  in the materials, confirming the point that photoemitted electrons originating from energies less than  $-2.0 \text{ eV}$  are excited from Cu  $d$  states, and indicating that the Cu  $d$  states are little changed with alloying.<sup>51</sup>

### C. Alloy Optical Densities of States

From the alloy photoemission data described above, optical densities of filled states have been obtained using the constant matrix element, non-direct-transition model discussed in Sec. IV. In applying the analysis of Sec. IV to the alloy data, the magnitude of the electron-electron scattering mean free path  $l_e$  was not used as an adjustable parameter to fit the experimental quantum yield, as was done in the case of pure Cu.<sup>20</sup> Rather,  $l_e$  in the alloys was taken to have the same magnitude as in pure Cu - about  $20 \text{ \AA}$  at  $10 \text{ eV}$  above  $E_F$ . In order to explain the increasing yield with increasing Ni content (Fig. 3), in terms of changes in  $l_e$  only,  $l_e$  would have to be greater in the alloys than in pure

Cu, which appears to be unrealistic. It seems plausible that the electron-electron scattering mean free path at high energies will not be greatly different in the alloys and pure Cu. Therefore, in applying the nondirect analysis to the alloy data, only the shape of the EDCs and yield have been fitted.

Calculations of alloy EDCs from the optical densities of states also included the effects of once-scattered electrons, calculated from the second term of Eq. (1). The scattered electron contribution accounted for only about 12.5% of the total quantum yield at  $h\nu = 11.4$  eV. As mentioned in Sec. IV, the inclusion of short elastic mean free path did not significantly affect the EDC calculations. The position of the free-electron-like band, used in the analysis to approximate the unfilled states and to calculate the surface escape probability, was not used as an adjustable parameter, but the bottom of this band was fixed 7 eV below  $E_F$ , as suggested by the free-electron model of Cu and Cu-band calculations.

The optical densities of states (ODS) obtained for 87% Cu and 77% Cu are shown in Fig. 11. The magnitudes of the two ODS relative to one another are arbitrary. For energies less than  $-2.0$  eV the densities of states bear a fairly close resemblance, in the energy position of structure at least, to the optical density of states for pure copper.<sup>20</sup> Between 0 and  $-2.0$  eV an increasing number of states, due to the Ni  $d$  electrons existing in virtual-bound-type levels, is present as the Ni content is increased. The existence of such states is clearly evident in the raw data (Fig. 10). In the raw data the relationship of the VBS peak to both the Cu  $d$ -state edge at about  $-2.0$  eV and the leading edge of the EDCs establishes that the center of the Ni  $d$  states is at about  $-1.0$  eV. The position and width of the Ni VBS will be discussed in

greater detail in Sec. VI. Below  $-4.0$  or  $-5.0$  eV the alloy optical densities of states are relatively uncertain because of the presence of large numbers of scattered electrons in the original data; therefore, this region is dashed to indicate the uncertainty. Theoretical calculations<sup>47</sup> of the Cu  $d$  states suggest that the Cu  $d$  states extend to only  $-5.5$  or  $-6.0$  eV.

The first structure in the Cu  $d$  states is greatly reduced in relative magnitude in the alloys compared to its strength in pure Cu.<sup>20</sup> This reduction may result because the states at the energy of the first Cu  $d$ -state peak overlap, and may interact with, the Ni virtual-bound levels; or the magnitude of this peak may be underestimated because of some loss of resolution in the heat-cleaned samples, or a combination of these effects.

As mentioned above, the density of empty states in the alloys has been approximated by a free-electron band,  $N_f(E) \propto \sqrt{E}$ , with the band bottom at  $-7.0$  eV. As will be discussed below, Ni VBS in Cu are only partially filled, containing approximately nine electrons, so just above  $E_F$  an additional number of states is indicated on the alloy densities of states to account approximately for the unfilled portion of the Ni VBS. No structure in the empty states at about  $+1.5$  eV is included in the alloy densities of states as in pure Cu<sup>20</sup> since no evidence for such structure has been found in our studies.

#### D. Reflectivity and Optical Parameters of Cu-Ni Alloys

In Fig. 12 the measured near-normal incidence reflectivities ( $R$ ) of the 87% Cu and 77% Cu alloys for photon energies between 0.5 and 11.8 eV are shown. Also shown in Fig. 12 is the reflectivity of pure copper; the reflectivity values for Cu are taken from previously unpublished measurements made by Donovan<sup>52</sup> in the energy range  $0.05 \leq h\nu \leq 8.0$  eV and from the measurements of Beaglehole<sup>34</sup> in the energy region  $8.0 \leq h\nu \leq 12.0$  eV. These measurements were made under conditions closely approximating those of the present alloy measurements and matched quite well in the vicinity of 8.0 eV.

By far the most pronounced change in the reflectivity spectra of the alloys compared to that of pure Cu occurs in the photon energy range 0–2.0 eV. The behavior of  $R$  for the three compositions in this energy range is shown in greater detail in the insert in Fig. 12. The reflectivity of Cu is near 100% and very flat until  $h\nu \cong 2.1$  eV, where there is a sharp drop. In the alloys, the reflectivity in the range  $h\nu = 0$  to 2.0 eV decreases with increasing Ni content. However, there is still a sharp drop in  $R$  at  $h\nu \cong 2.1$  eV for the 87% Cu alloy and the 77% Cu alloy reflectivity exhibits a rapid,

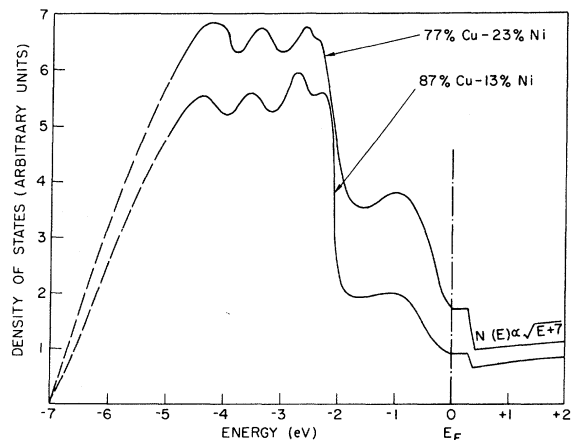


FIG. 11. ODS for 87% Cu-13% Ni and 77% Cu-13% Ni.

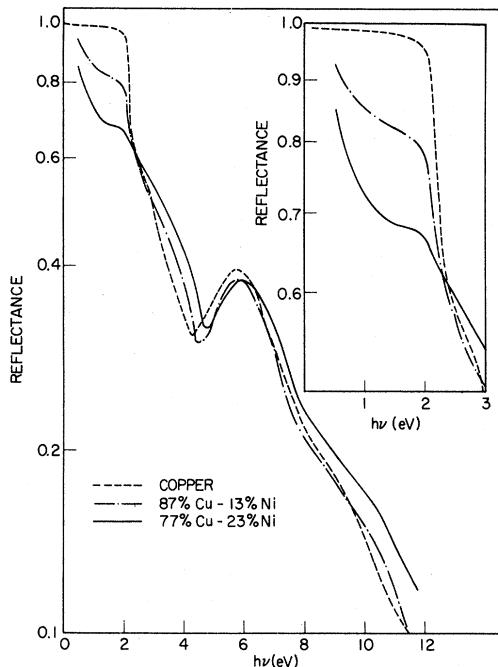


FIG. 12. Reflectivity for pure Cu, 87% Cu, and 77% Cu. The insert shows the low- $h\nu$  behavior. The reflectivity for Cu is from Refs. 34 and 52.

though not so steep, decline beyond 2.0 eV. The sharp drop in reflectivity of pure Cu at  $h\nu \approx 2.1$  eV is due to the onset of strong transitions from the Cu  $d$  states to  $E_F$ . The fact that there is a sharp drop in reflectivity in the 87% Cu and 77% Cu alloys at  $h\nu \approx 2.1$  eV indicates, as did the photoemission data, that the Cu  $d$ -state to  $E_F$  separation remains the same in Cu and Cu-rich Cu-Ni alloys. Schröder and Öngüt,<sup>11</sup> in interpreting their absorptivity measurements on Cu-Ni alloys to 25% Ni, have previously established this same point. The results of Schröder and Öngüt,<sup>11</sup> while not as sharp, are in good agreement with the present data. Also, the reflectivity spectrum obtained by Scouler, Feinleib, and Hanus<sup>14</sup> for an alloy of composition 84% Cu-16% Ni is completely consistent with the present results.

Another change in the reflectivity spectra with increasing Ni content is a shift of the local minimum at 4.3 eV in pure Cu to about 4.8 eV in the 77% Cu alloy. The peak in the vicinity of 5.8 eV shifts only very slightly upon alloying.

In Fig. 13, the optical transition strength  $\omega\sigma$  is shown for Cu and the two Cu-Ni alloys studied. The optical transition strength for Cu between  $h\nu = 0$  and 2.0 eV, which is due to Drude or free-electron absorption, is weak. At  $h\nu \approx 2.1$  eV,  $\omega\sigma$  for Cu increases rapidly because of  $d$ -band  $\rightarrow E_F$  transitions and beyond this absorption edge there is

pronounced structure in the vicinity of 5.4 eV. The addition of Ni to Cu causes a large increase in the absorption between 0 and 2.0 eV. The  $\omega\sigma$  curves for 87% Cu and 77% Cu have distinct peaks at  $h\nu = 1.3$  eV and  $h\nu = 1.8$  eV, respectively, and the relative strength of this structure increases with increasing Ni content. Beyond 3.0 eV,  $\omega\sigma$  is quite similar for the three materials; a slight shift of the peak in the vicinity of  $h\nu = 5.4$  eV to higher energies as the Ni content of the alloys increases is evident.

The additional optical absorption in the Cu-Ni alloys for  $0 \leq h\nu \leq 2.0$  eV must be due to the presence of Ni virtual-bound levels between  $E_F$  and the Cu  $d$  states. The photoemission data of Sec. V B indicate that the Ni virtual-bound levels give appreciable  $d$ -state density between the Fermi level and the Cu  $d$  states, so a significant contribution to the optical absorption from the Ni  $d$  states can result for all photon energies.

## VI. DISCUSSION OF RESULTS

From the Cu-Ni alloy EDCs and ODS, it has been established that a VBS type of model describes the Ni  $d$  states in Cu-rich Cu-Ni alloys and that the Cu  $d$  states in Cu-rich Cu-Ni alloys are little changed, with regard to the energy position of structure, from the  $d$  states in pure Cu. In addition to these qualitative conclusions, it is of interest to attempt a more detailed analysis of the VBS of Ni in Cu in order to obtain an estimate of its position, width, and the relative importance of  $s$ - $d$  and  $d$ - $d$  interactions in determining the width. While the values of the VBS width obtained in the analysis below will be somewhat uncertain because it is not known how

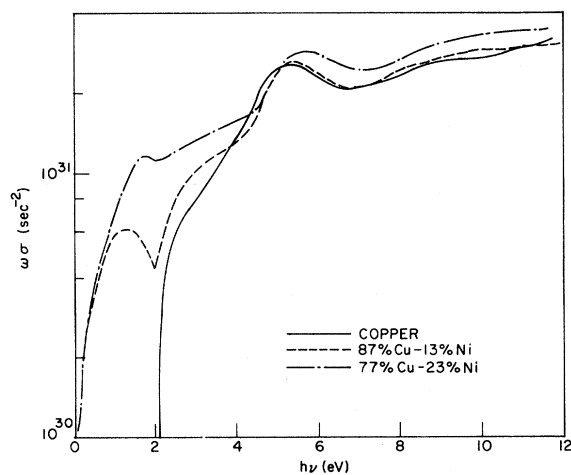


FIG. 13. Optical transition strength  $\omega\sigma$  for Cu and Cu-Ni alloys. Ni virtual-bound levels produce a very pronounced change for  $0 \leq h\nu \leq 2.0$  eV.

to correct these values for experimental resolution effects, such an analysis appears to be useful at this time because of the lack of more direct data on the VBS of Ni in Cu.

In treating the VBS problem, Anderson<sup>18</sup> and Klein and Heeger<sup>10</sup> found that the density of  $d$ -state admixture,  $\rho_d(E)$ , in a nearly free-electron-like band per transition-metal impurity atom is given by the expression

$$\rho_d(E) = \frac{10}{\pi} \frac{\Delta_{sd}}{(E - E_d)^2 + \Delta_{sd}^2} \quad (3)$$

Here  $E_d$  is the energy position of the VBS and  $\Delta_{sd}$  is the energy half-width at half-maximum of the level due to the mixing of the impurity  $d$  states with the nearly free-electron-like states of the host. Equation (3) describes the situation when the spin-up and spin-down VBS are not split in energy; magnetic-susceptibility data for Cu-Ni alloys<sup>26,53</sup> indicate that for Ni concentrations less than about 40% this situation applies.

Equation (3) (and in the strictest sense, the VBS model itself) cannot be expected to be completely valid for describing the rather concentrated alloys studied here since this model was originally formulated to deal with isolated noninteracting impurities. However, the VBS model and Eq. (3) provide a logical starting point for analyzing the present data for several reasons. First of all, the alloy data are in agreement with the qualitative predictions of this model, as discussed previously. Second, one of the most important parameters of the VBS model is the interaction between the  $d$  states of the impurity atom and the nearly free-electron-like states of the host material. This interaction is almost always neglected in tight-binding<sup>54</sup> and multiple-scattering treatments<sup>55</sup> of the  $d$  states in transition-metal alloys, yet measurements on very dilute Cu-Mn<sup>56</sup> alloys indicate that this interaction can give appreciable energy width to the impurity  $d$  states. It is also found below that most of the energy width of the Ni  $d$  states in the Cu-Ni alloys studied here is given by this  $s$ - $d$  interaction. Therefore, the VBS theory incorporates an important effect which is neglected in other theoretical models which treat alloys similar to Cu-Ni. (The tight-binding and multiple-scattering models of alloys do have certain features in common with the VBS model, such as the prediction of separate host and impurity  $d$  levels when the atomic-energy levels are well separated.) Finally, concentration effects, or effects which occur when the added impurities can no longer be assumed to be noninteracting, have been incorporated into the original VBS model by Kim.<sup>57</sup> This treatment suggests that for nondilute alloys the

Lorentzian form of Eq. (3) will remain approximately valid but the energy position and width of the VBS may depend upon the solute concentration. Therefore, evaluation of the VBS parameters at different alloy compositions can give information concerning the concentration effects which are present.

An estimate of the parameters  $E_d$  and  $\Delta_{sd}$  of Eq. (3) for the Ni VBS in Cu can be obtained by considering the Ni  $d$ -state contribution to the EDCs for 87% Cu and 77% Cu. In obtaining this contribution in the range of initial-state energies from 0 to -2.0 eV, it is necessary to take into account the contribution of the  $s$ - and  $p$ -derived electrons excited in this same energy range. These electrons give an important contribution to the total number of photoemitted electrons for initial-state energies between 0 and -2.0 eV, especially in the 87% Cu alloy.

The procedure which we have adopted to approximately obtain the Ni VBS contribution to the alloy EDCs is to use the EDCs obtained for pure Cu in the present work to give a measure of the  $s$ - and  $p$ -like electron contribution to the alloy EDCs. That is, at a particular  $h\nu$ , scaled values of the number of electrons photoemitted from pure Cu are subtracted from the number of electrons photoemitted from the alloy in the initial-state energy range of 0 to -2.0 eV. This procedure then involves the assumption that the behavior with  $h\nu$  of the photoemitted  $s$ - and  $p$ -like electrons is the same in the alloys as in pure Cu. The photoemission results of Norris and Nilsson<sup>58</sup> on Ag-Pd alloys clearly show that a contribution from  $s$ - and  $p$ -derived electrons, almost identical to that in pure Ag, is present in EDCs for an alloy containing 85% Ag-15% Pd. Therefore, the above assumption does not seem unreasonable.

The absolute quantum yields, and hence the absolute magnitude of the normalized EDCs, increase with increasing Ni content. Therefore, the values of the pure Cu EDCs must be adjusted so as to put the Cu and alloy curves on equivalent scales before subtraction. The pure Cu curves have been adjusted by matching the height of the first Cu  $d$ -state peak at about -2.5 eV to the height of the equivalent peak in the alloy EDCs. Although the height of the -2.5-eV structure in the alloy EDCs appears to be somewhat smaller relative to other structure than in pure Cu, this process gives a reasonably good basis for comparison.

The above procedure has been followed for 17 EDCs for 87% Cu-13% Ni and 20 EDCs for 77% Cu-23% Ni. Some typical results for the Ni VBS contribution to the 87% Cu EDCs are shown in Fig. 14. These particular curves were chosen to illustrate the behavior over a wide range of photon

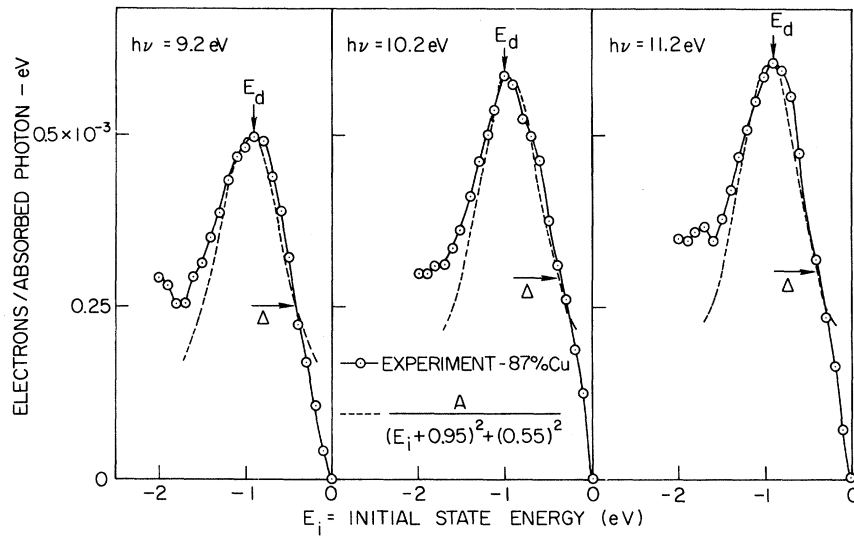


FIG. 14. Ni  $d$ -state contribution to 87% Cu alloy EDCs, showing experimental contribution and that calculated from the VBS expression [Eq. (3)] and experimentally deduced parameters. Agreement is very good, except near  $-2$  eV.

energies; the results for other  $h\nu$  were essentially identical to the curves shown. The solid, or experimental, curves are obtained by the procedure above and closely resemble Lorentzian-shaped peaks, with the major deviations occurring near  $-2$  eV, where the presence of the Cu  $d$  states may modify the form of the VBS or affect the shape of the EDCs. The experimental curves indicate that the Ni  $d$ -state contribution to the density of states goes to zero at 0 eV (the Fermi energy); however, this is a consequence of the experimental resolution. Actually, the Fermi level cuts the Ni VBS so that it contains only about nine  $d$  electrons and so that there is appreciable Ni  $d$ -state density at the Fermi level.

Values of  $E_d$ , the position of the peak, and the half-width at half-maximum of the Ni  $d$  states,  $\Delta$ , measured to the right as shown, can be determined from the curves of Fig. 14 and the curves obtained for other  $h\nu$ . Here  $\Delta$  is defined as the sum of  $\Delta_{sd}$ , the energy width of the Ni  $d$  states due to  $s$ - $d$  interaction alone, and any contribution due to interaction of VBS on different Ni atoms. It is assumed that the shape of the Ni  $d$  states in 87% Cu-13% Ni is given by Eq. (3) with  $\Delta$  replacing  $\Delta_{sd}$ . The average values for  $E_d$  and  $\Delta$  obtained from 17 different curves for 87% Cu are  $E_d = -0.95 \pm 0.05$  eV and  $\Delta = 0.55 \pm 0.05$  eV. Also shown on Fig. 14 is the curve calculated using the experimentally deduced parameters and the appropriate form of Eq. (3):

$$\rho_d(E_i) = A / [(E_i + 0.95)^2 + (0.55)^2],$$

where  $E_i$  is the initial-state energy and  $A$  is a constant chosen to match the peak height of the experimental curves. The calculated curves are seen to match the shape to the experimental curves

very well, particularly in the vicinity of  $-1.0$ .

Repeating the above process for the 77% Cu EDCs yields the typical results for the Ni VBS contribution to these EDCs shown in Fig. 15. Again peaked structures are obtained, although they are somewhat unsymmetrical about the peak position. Defining  $E_d$  and  $\Delta$  as before, the average values  $E_d = 1.0 \pm 0.05$  eV and  $\Delta = 0.65 \pm 0.05$  eV are obtained from 20 curves. The curve defined by

$$\rho_d(E_i) = A / [(E_i + 1.0)^2 + (0.65)^2]$$

is also shown in Fig. 15, and the agreement is fairly good except near  $-2.0$  eV.

The difference in the values of  $\Delta$  obtained for the 87% Cu and 77% Cu alloys (0.55 and 0.65 eV, respectively) suggests that the width of the Ni  $d$ -state density varies with concentration because of the interaction of VBS on different solute atoms. Therefore, as anticipated above, it is necessary to go beyond the simplest form of the VBS model in order to more completely describe the behavior of the Ni  $d$  states with increasing concentration.

Kim<sup>57</sup> has extended Anderson's<sup>18</sup> theory of the VBS to include interactions between the solute atoms to lowest order in the concentration. Kim's<sup>57</sup> treatment indicates that the VBS width should vary linearly with concentration. The concentration-dependent portion of the width arises predominately from an indirect interaction between impurities, i. e., through a process in which a Ni  $d$  electron in a VBS undergoes a transition to a free-electron-like state, is scattered by another Ni atom, and then returns to the initial state. Beeby<sup>54</sup> has given a tight-binding theory of alloying behavior which also indicates that the solute bandwidth varies linearly with composition. Model calculations, based on the coherent-potential approxi-

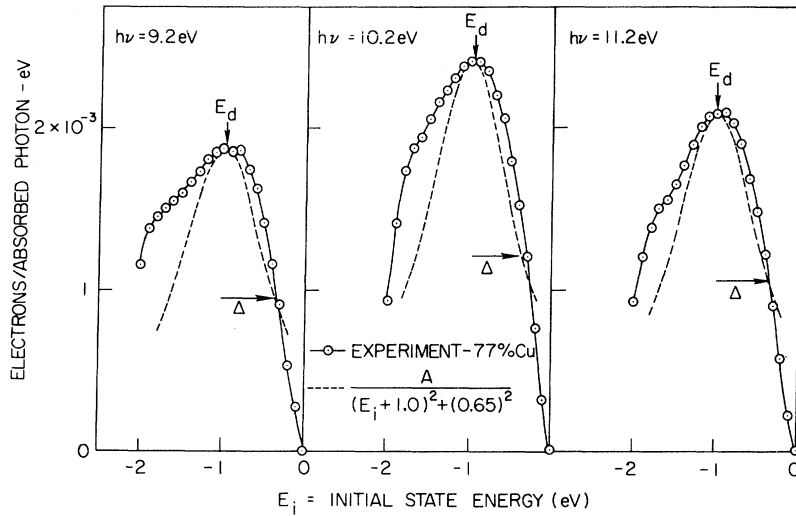


FIG. 15. Ni *d*-state contribution to 77% Cu alloy EDCs, showing experimental contribution and that calculated from the VBS expression [Eq. (3)] and experimentally deduced parameters. The major disagreement again occurs near  $-2.0$  eV.

mation by Velický, Kirkpatrick, and Ehrenreich,<sup>55</sup> indicate that solute bandwidth varies somewhat faster than linearly – as  $c^{1/2}$  – but the assumptions of the coherent-potential approximation overestimate the bandwidth. Neither of the latter two treatments includes *s-d* interactions.

If we assume that the alloy compositions studied here are still in the range of concentrations where a linear dependence of bandwidth on concentration holds, then the energy width of the Ni VBS  $\Delta(c)$  can be represented as

$$\Delta(c) = \Delta_{sd} + c\Delta_{dd} \quad (4)$$

Here  $\Delta_{dd}$  is a coefficient containing all contributions to the change in solute bandwidth which are linear in concentration.<sup>59</sup> Using the two measured values of  $\Delta$  for the 87% Cu and 77% Cu alloys, Eq. (4) can be readily solved for  $\Delta_{sd}$  and  $\Delta_{dd}$ . The resulting values are

$$\Delta_{sd} = 0.42 \pm 0.05 \text{ eV}; \quad \Delta_{dd} = 1 \text{ eV}.$$

This final value for  $\Delta_{sd}$  indicates that the major portion of the Ni VBS width in 87% Cu and 77% Cu is due to *s-d* interactions, although the interaction of states on different Ni atoms is also important for these compositions.

As cautioned previously, the values of  $\Delta$  and  $\Delta_{sd}$  obtained above may be too large because of experimental broadening. A rough estimate of the increase in measured width due to broadening can be obtained by assuming the experimental broadening is a Gaussian function of total width at half-maximum of 0.4 eV. Convoluting this broadening function with a Lorentzian VBS with  $\Delta = 0.5$  eV [(Eq. (3))] results in a structure with a half-width at half-maximum of 0.57 eV. This suggests that the measured  $\Delta$  values and  $\Delta_{sd}$  are high by at most 20%, owing to experi-

mental broadening.

While it is clear that some degree of subtraction of the *s-p* contribution to alloy EDCs in the region of the Ni VBS is necessary, the values of  $\Delta$  obtained are somewhat sensitive to the manner in which the pure Cu and alloy EDCs are scaled before subtraction. This fact also affects the accuracy of the deduced value of  $\Delta_{sd}$ . If no subtraction were done, a width of  $\Delta = 0.75 \pm 0.05$  eV would result for the Ni VBS in both 87% Cu and 77% Cu, suggesting that *d-d* interactions do not affect the VBS width. The value  $\Delta_{dd} = 1$  eV obtained using subtraction therefore constitutes an approximate upper limit on the magnitude of the *d-d* interaction effect. In either case, the conclusion that *s-d* interactions contribute most of the width of the Ni VBS in Cu for the compositions studied remains valid.

A summary of the present determination of  $E_F - E_d$  and  $\Delta_{sd}$  for Ni VBS in Cu is shown in Table I. The presence of VBS in an alloy can greatly affect the properties of that alloy; Klein and Heeger<sup>10</sup> have discussed in detail the effect of the VBS on the electronic specific heat, magnetic susceptibility, and resistivity of an alloy. A VBS in which spin-up and spin-down states are not split and which is only partially filled will cause an increase in resistivity and electronic specific heat and will also contribute a temperature-independent paramagnetism. Therefore, measurements of these and similar properties of Cu-Ni alloys have previously been used to deduce  $E_F - E_d$  and  $\Delta_{sd}$  for the VBS of Ni in Cu. Shown in Table I are determinations of these parameters obtained by Foiles<sup>13</sup> from thermoelectric-power measurements and by Klein and Heeger<sup>10</sup> from residual resistivity and low-temperature specific-heat measurements. Both of these latter determinations are rather in-

TABLE I. Determinations of VBS Parameters for Ni in Cu.

| Method and source   | $E_F - E_d$ (eV) | $\Delta_{sd}$ (eV)     | Composition | Comment  |
|---|------------------|------------------------|-------------|--|
| Photoemission – present work  | $0.95 \pm 0.05$  | $0.42 \pm 0.05$        | 13%, 23% Ni | Ni $d$ -state width taken to vary linearly with composition  |
| Thermoelectric power – Foiles (Ref. 13)                             | $0.70 \pm 0.05$  | $0.25 \pm 0.1$         | < 1% Ni     | Lorentzian:<br>$\rho_d(E) \propto \frac{\Delta_{sd}}{(E - E_d)^2 + \Delta_{sd}^2}$   |
|   | $1.35 \pm 0.1$   | $\Sigma = 1.3 \pm 0.1$ | < 1% Ni     | Gaussian:<br>$\rho_d(E) \propto \exp[-(E - E_d)^2 / 2\Sigma^2]$  |
| Specific heat and residual resistivity – Klein and Heeger (Ref. 10) | $\sim 0.93$      | $\sim 0.3$             | 10% Ni      | Assumes linear variation of the electronic specific-heat coefficient with concentration between 0 and 10% Ni; does not include variation of $\Delta$ with composition. |
| Specific heat and photoemission – present work and Ref. 7           | 0.95             | 0.56                   | 10% Ni      |  |

direct, as they involve measurements of electronic properties at or near the Fermi surface only, and depend upon the Ni  $d$ -state density at the Fermi level being exactly as given by Eq. (3). The thermoelectric-power data<sup>13</sup> can only be related to the VBS model through several additional approximations: The sensitivity of the parameters to these approximations and the exact shape of the nickel states is illustrated in the table where a Gaussian form  $\exp[-(E_i - E_d)^2 / 2\Sigma^2]$  was assumed and quite different parameter values resulted. Klein and Heeger<sup>10</sup> give only a very rough estimate of  $\Delta_{sd}$  from the specific-heat data. We have reanalyzed the specific-heat data<sup>7</sup> and find, using  $E_F - E_d = 0.95$  eV as obtained from the photoemission data, that  $\Delta_{sd} = 0.56$  eV. This value is somewhat larger than the value obtained from the photoemission data, but the derivation of  $\Delta_{sd}$  from specific-heat data does not include concentration effects, which may explain the discrepancy.

Integrating Eq. (3) from  $-\infty$  to  $E_F$  using the VBS parameters given in Table I implies that each Ni VBS contains about nine  $d$  electrons, quite close to the number of  $d$ -like electrons found in pure Ni.

In addition to those experimental results for copper-nickel alloys noted in Table I, other data for these alloys have been found to be consistent with the VBS model. Klein and Heeger<sup>10</sup> note that the magnetic susceptibility and residual resistivity of dilute Cu-rich Cu-Ni alloys is understandable in terms of the VBS model. Schröder and Öngüt have interpreted optical-absorptivity data of Cu-Ni alloys to 25% Ni in terms of VBS model, and Chollet and Templeton<sup>12</sup> have concluded from de Haas-van Alphen measurements of very dilute Cu-Ni alloys

that the Ni  $d$  electrons exist in virtual-bound levels.

## VII. SUMMARY AND CONCLUSIONS

As discussed above, the VBS model, modified to include concentration effects, is able to account for the important changes in photoemission data which occur when moderate amounts of Ni are alloyed with Cu. The VBS model also provides a means for understanding other properties of Cu-Ni alloys which were inconsistent with the rigid-band model. Photoemission and/or optical studies have shown that the VBS model is also appropriate for describing the electronic structure of many other noble-metal-transition-metal alloy systems.<sup>58, 60, 61</sup>

The fact that Cu and Ni  $d$ -like electrons form independent, essentially noninteracting levels occurs because the  $d$ -scattering resonances in the vicinity of Ni and Cu atoms are fairly widely separated in energy. In a Cu-rich Cu-Ni alloy, each Cu or Ni core in the alloy tends to be surrounded by very nearly the same electronic configuration as in pure Cu or pure Ni, respectively; there is no appreciable transfer of electrons from Cu to Ni sites to fill the Ni  $d$  states as rigid- or common-band models would suggest. Our analysis of the width of the Ni  $d$  states in Cu-rich Cu-Ni alloys suggests that the interactions among states on different Ni atoms broaden the Ni  $d$  states at the rate of approximately 0.01 eV per atomic percent Ni. The deviations of the experimentally deduced Ni  $d$ -state density for 77% Cu from the ideal VBS form (Fig. 15) also suggest that the interactions among Ni atoms begin to modify the shape of the Ni  $d$ -state density at this concentration. The observation that interaction effects are appreciable is not surprising – for very dilute Ni concen-



trations the  $d$ -state density has a total half-width of about 1.0 eV, which must increase to 4–5 eV in 100% Ni because of interaction effects. The fact that the Cu  $d$  states remain more than 2.0 eV below  $E_F$  in Cu-rich Cu-Ni alloys appears to also hold true in more concentrated Ni alloys, as will be established in the succeeding paper.<sup>22</sup>

Optical transitions in the alloys studied here are almost certainly nondirect in nature. This conclusion is based upon the success of the nondirect model in explaining the alloy results, upon the disappearance of the  $L_2' \rightarrow L_1$  direct transition in the alloys,<sup>21</sup> and also upon the fact that, since Cu and Ni  $d$ -derived electrons do not share common bands, the resultant distortion of the  $d$ -derived wave functions will tend to remove  $\vec{k}$  as a meaningful quantum number and hence invalidate the  $\vec{k}$  selection rule. Further discussion of the nature of optical transitions in Cu and Cu-Ni alloys is deferred until after

results for several more Cu-Ni alloys and pure Ni are given in the following paper.

#### ACKNOWLEDGMENTS

The authors are grateful to Dr. R. Smoluchowski for first pointing out the problem of possible clustering in the Cu-Ni alloys, and to Dr. S. C. Moss, Dr. J. S. Kouvel, Dr. P. A. Beck, and Dr. J. B. Cohen for pertinent discussions and communications regarding the clustering problem. We are also grateful to Dr. Ray R. Dils for arranging the microprobe analysis of one of our samples. We thank Dr. H. Ehrenreich, Dr. S. Kirkpatrick, and Dr. D. J. Kim for communicating their results, concerning the minimum-polarity model of Cu-Ni alloys and solute-concentration effects, respectively, prior to publication. Finally, we acknowledge helpful and stimulating discussions with Dr. W. A. Harrison and Dr. A. Bienenstock.

\*Work supported by the National Science Foundation and the Advanced Research Projects Agency through the Center for Materials Research at Stanford University, Stanford, Calif.

<sup>†</sup>NSF trainee, part of work submitted for the Ph. D. degree in Electrical Engineering. Present address: The Aerospace Corp., El Segundo, Calif.

<sup>1</sup>M. Adler, thesis, Zurich, 1916 (unpublished), quoted by N. F. Mott, Proc. Phys. Soc. (London) 47, 571 (1935).

<sup>2</sup>H. Lowery, J. Bor, and H. Wilkinson, Phil. Mag. 20, 390 (1935).

<sup>3</sup>N. F. Mott, Proc. Phys. Soc. (London) 47, 571 (1935); Phil. Mag. 22, 287 (1936).

<sup>4</sup>A. Kidron, Phys. Rev. Letters 22, 774 (1969).

<sup>5</sup>B. R. Coles, Proc. Phys. Soc. (London) B65, 221 (1952), gives excellent summary of experimental and theoretical situation prior to 1952.

<sup>6</sup>E. W. Pugh and F. M. Ryan, Phys. Rev. 111, 1038 (1958).

<sup>7</sup>G. L. Guthrie, S. A. Friedberg, and J. E. Goldman, Phys. Rev. 113, 45 (1959).

<sup>8</sup>J. Clift, C. Curry, and B. J. Thompson, Phil. Mag. 8, 593 (1963).

<sup>9</sup>K. P. Gupta, C. H. Cheng, and P. A. Beck, Phys. Rev. 113, A203 (1964).

<sup>10</sup>A. P. Klein and A. J. Heeger, Phys. Rev. 144, 458 (1966).

<sup>11</sup>K. Schröder and D. Öngüt, Phys. Rev. 162, 628 (1967).

<sup>12</sup>L.-F. Chollet and I. M. Templeton, Phys. Rev. 170, 656 (1968).

<sup>13</sup>C. L. Foiles, Phys. Rev. 169, 471 (1968).

<sup>14</sup>W. Scouler, J. Feinleib, and J. Hanus, J. Appl. Phys. 40, 1400 (1969).

<sup>15</sup>N. D. Lang and H. Ehrenreich, Phys. Rev. 168, 605 (1968).

<sup>16</sup>C. G. Robins, H. Claus, and P. A. Beck, Phys. Rev. Letters 22, 1307 (1969); J. Appl. Phys. 40, 2269 (1969).

<sup>17</sup>J. Friedel, Can. J. Phys. 34, 1190 (1956); J. Phys.

Radium 19, 573 (1958).

<sup>18</sup>P. W. Anderson, Phys. Rev. 124, 41 (1961).

<sup>19</sup>C. N. Berglund and W. E. Spicer, Phys. Rev. 136, A1030 (1964); 136, A1045 (1964).

<sup>20</sup>W. Krolikowski and W. E. Spicer, Phys. Rev. 185, 882 (1969).

<sup>21</sup>D. H. Seib and W. E. Spicer, Phys. Rev. Letters 20, 1441 (1968); 22, 711 (1969); Phys. Rev. 187, 1176 (1969); L. E. Walldén, D. H. Seib, and W. E. Spicer, J. Appl. Phys. 40, 1281 (1969).

<sup>22</sup>D. H. Seib and W. E. Spicer, following paper, Phys. Rev. B 2, 1694 (1970).

<sup>23</sup>B. Mozer, D. T. Keating, and S. C. Moss, Phys. Rev. 175, 868 (1968).

<sup>24</sup>J. W. Cable, E. O. Wollan, and H. R. Child, Phys. Rev. Letters 22, 1256 (1969).

<sup>25</sup>H. C. Van Elst, B. Lubach, and G. J. Van Den Berg, Physica 28, 1297 (1962).

<sup>26</sup>F. M. Ryan, E. W. Pugh, and R. Smoluchowski, Phys. Rev. 116, 1106 (1959).

<sup>27</sup>S. K. Dutta Roy and A. V. Subrahmanyam, Phys. Rev. 177, 1133 (1969).

<sup>28</sup>T. J. Hicks, B. Rainford, J. S. Kouvel, G. G. Low, and J. B. Comly, Phys. Rev. Letters 22, 531 (1969).

<sup>29</sup>L. H. Bennett, L. J. Swartzendruber, and R. E. Watson, Phys. Rev. Letters 23, 1171 (1969).

<sup>30</sup>S. C. Moss, Phys. Rev. Letters 23, 381 (1969).

<sup>31</sup>I. S. Brammar and M. A. P. Dewey, *Specimen Preparation for Electron Metallography* (American Elsevier, New York, 1966), p. 65.

<sup>32</sup>R. M. Brick and A. Phillips, *Structure and Properties of Alloys* (McGraw-Hill, New York, 1949), pp. 57, 88.

<sup>33</sup>S. Roberts, Phys. Rev. 118, 1509 (1960).

<sup>34</sup>D. Beaglehole, Proc. Phys. Soc. (London) 85, 1007 (1965); 87, 461 (1966).

<sup>35</sup>G. W. Simmons, D. F. Mitchell, and K. R. Lawless, Surface Sci. 8, 130 (1967).

<sup>36</sup>W. E. Spicer and C. N. Berglund, Rev. Sci. Instr. 35, 1665 (1964).

<sup>37</sup>R. C. Eden, Rev. Sci. Instr. 41, 252 (1970).

<sup>38</sup>R. Koyama, Ph. D. thesis (unpublished); Stanford Electronics Laboratory Technical Report No. 5223-1, Stanford University, 1969 (unpublished).

<sup>39</sup>A. Y-C. Yu, T. M. Donovan, and W. E. Spicer, Phys. Rev. 167, 670 (1968).

<sup>40</sup>W. E. Spicer, Phys. Rev. Letters 11, 243 (1963).

<sup>41</sup>D. E. Eastman and W. Krolikowski, Phys. Rev. Letters 21, 623 (1968).

<sup>42</sup>N. Smith and W. E. Spicer, Opt. Commun. 1, 157 (1969); N. Smith, Phys. Rev. Letters 23, 1452 (1969).

<sup>43</sup>W. E. Spicer, J. Res. Natl. Bur. Std. 74A, 397 (1970).

<sup>44</sup>S. Doniach (private communication).

<sup>45</sup>S. W. Duckett, Phys. Rev. 166, 302 (1968).

<sup>46</sup>L. Hodges, H. Ehrenreich, and N. D. Lang, Phys. Rev. 152, 505 (1966).

<sup>47</sup>F. C. Snow, Phys. Rev. 171, 785 (1968).

<sup>48</sup>F. Stern, *Solid-State Physics*, edited by F. Seitz and D. Turnbull (Academic, New York, 1963), Vol. 15.

<sup>49</sup>Further details of the Kramers-Krönig analysis procedure and a compilation of all of the deduced optical parameters can be found in D. H. Seib's Ph. D. thesis [Stanford University, 1969 (unpublished)] which may be obtained by writing University Microfilms, 300 N. Zeeb Road, Ann Arbor, Mich. 48106.

<sup>50</sup>R. H. Fowler, Phys. Rev. 38, 45 (1931).

<sup>51</sup>The fact that there are compositional inhomogeneities in the 77% Cu alloy due to the dendritic growth process (Sec. III) strongly supports the above conclusion concerning the constant  $E_F$  to Cu  $d$ -state energy separation. If the Cu  $d$ -state to  $E_F$  energy separation varied with composition, then the EDC structure, particularly the edge near  $-2.0$  eV, would be smeared out because of the presence of regions of differing composition. The fact that the Cu  $d$ -band edge remains fairly sharp in 77% Cu despite the known compositional variation excludes

the possibility of strong variation of the Cu  $d$ -state to  $E_F$  energy separation with composition.

<sup>52</sup>T. M. Donovan (private communication).

<sup>53</sup>E. Vogt, *Physikalische Eigenschaften Der Metalle, Band I* (Akademische Verlagsgesellschaft, 1958), p. 240.

<sup>54</sup>J. L. Beeby, Phys. Rev. 135, A130 (1964).

<sup>55</sup>B. Velický, S. Kirkpatrick, and H. Ehrenreich, Phys. Rev. 175, 747 (1968).

<sup>56</sup>J. A. McElroy and A. J. Heeger, Phys. Rev. Letters 20, 1481 (1968).

<sup>57</sup>D. J. Kim (private communication); Phys. Rev. B 1, 3725 (1970); D. J. Kim and Y. Nagaoka, Progr. Theoret. Phys. (Koyoto) 30, 743 (1963).

<sup>58</sup>C. Norris and P. O. Nilsson, Solid State Commun. 6, 649 (1968).

<sup>59</sup>As written, Eq. (4) implies that the VBS width due to  $s$ - $d$  interactions,  $\Delta_{sd}$ , does not change with concentration. However, if the density of free-electron-like states available for mixing with the Ni  $d$  states changes as the Ni content increases,  $\Delta_{sd}$  could change [ $\Delta_{sd} \propto \rho_f(E)$ , where  $\rho_f(E)$  is the free-electron-like density of states]. If the change in  $\rho_f(E)$  is proportional to  $c$ , then Eq. (4) should be written as

$$\Delta(c) = (1 - \beta c) \Delta_{sd}^0 + c \Delta_{dd}',$$

where  $\beta$  is a constant of proportionality,  $\Delta_{dd}'$  is the width due to Ni interactions only, and  $\Delta_{sd}^0$  is the VBS width at extremely dilute concentrations. However, this form obviously reduces to Eq. (4), with  $\Delta_{dd} = \Delta_{dd}' - \beta \Delta_{sd}^0$ , and therefore the same value for  $\Delta_{sd}^0$ , the parameter of major interest, results from either form.

<sup>60</sup>F. Abelés, J. Phys. Radium 23, 677 (1962).

<sup>61</sup>Å. Karlsson, H. P. Myers, and L. Walldén, Solid State Commun. 5, 971 (1967); Phil. Mag. 18, 725 (1968); and private communication.